ELSEVIER

Earth and Planetary Science Letters 198 (2002) 371–380

EPSL

www.elsevier.com/locate/epsl

Mantle transition-zone structure beneath the South Pacific Superswell and evidence for a mantle plume underlying the Society hotspot

Fenglin Niu [a,*], Sean C. Solomon [a], Paul G. Silver [a], D. Suetsugu [b], H. Inoue [c]

[a] *Department of Terrestrial Magnetism, Carnegie Institution of Washington, 5241 Broad Branch Road, N.W., Washington, DC 20015, USA*

[b] *International Institute of Seismology and Earthquake Engineering, Building Research Institute, Tatehara 1, Tsukuba, Ibaraki 305-0802, Japan*

[c] *Solid Earth Science Division, National Research Institute for Earth Science and Disaster Prevention, Tennodai 3-1, Tsukuba, Ibaraki 305-0006, Japan*

Received 21 October 2001; received in revised form 4 February 2002; accepted 5 February 2002

Abstract

Underside reflections of shear waves from the discontinuities at 410 and 660 km depth are used to map lateral variations in the thickness of the mantle transition zone beneath the South Pacific Superswell and surrounding regions. Differential travel times of reflected waves indicate that the transition zone is about 25 km thinner than normal, and thus hotter than normal, over an area 500 km or less in diameter beneath the Society hotspot. There is no general difference, however, in transition-zone thickness between the Superswell area and its surroundings. Our observations support the inference that the thermal flux from lower to upper mantle beneath the South Pacific Superswell occur on the lateral scale of a mantle plume (several hundred kilometers) rather than that of a superplume (several thousand kilometers).

Keywords: superswells; superplumes; plumes; SS-waves; precursors; mantle; transition zones

1. Introduction

An area of anomalously shallow sea floor in the South Pacific several thousand kilometers in lateral extent (Fig. 1) is known as the South Pacific Superswell [1]. The superswell region includes four prominent linear chains of volcanic islands and seamounts terminating at their east–southeastern ends at the Marquesas, Pitcairn, Society, and Macdonald (Austral) hotspots (Fig. 1). Because several of these chains are characterized by a diffuse distribution of volcanic centers, complicated age relationships, or limited histories of volcanic activity [2–5], it is not clear which of these island and seamount groups were produced by the motion of the Pacific plate over classical mantle plumes [6] and which may be the result of only shallow magmatic processes. Global seismic tomography has revealed a long-wavelength low-

* Corresponding author. Tel.: +1-202-478-8837; Fax: +1-202-478-8821.
E-mail address: niu@dtm.ciw.edu (F. Niu).

0012-821X/02/$ – see front matter
PII: S0012-821X(02)00523-X

velocity anomaly in the lower mantle beneath the Pacific Superswell region, a feature that has been variously termed the Equatorial Pacific Plume Group [7] or the Pacific Superplume [8]. Global tomography, however, lacks the horizontal resolution to image individual plumes. The issue of whether a superswell is the product of broad upwelling of hot material in the upper mantle [9] or of comparably broad upwelling of a lower mantle superplume [10] is currently an open one.

In the absence of a local network of densely spaced seismic stations to image directly the upper mantle seismic velocity signature of a hot upwelling plume [11], mapping the lateral variation in the thickness of the mantle transition zone is an effective method for discerning whether a hotspot is underlain by a plume originating in the lower mantle [12,13]. The two prominent seismic discontinuities at 410 and 660 km depth are thought to be caused by the temperature-sensitive phase transitions from α-$(Mg,Fe)_2SiO_4$ to β-$(Mg,Fe)_2SiO_4$ [14] and from γ-$(Mg,Fe)_2SiO_4$ to perovskite plus magnesiowüstite [15], respectively. Because the two transitions have positive and negative Clapeyron slopes, respectively, an increase in temperature results in an increase in the depth to the 410-km discontinuity and a decrease in the depth to the 660-km discontinuity. Lateral variations in the transition-zone thickness, as well as variations in the depths of the two discontinuities, provide key information on lateral differences in mantle temperature at 400–700 km depth and thus on the nature of mantle plumes penetrating that depth range.

2. Data and analysis

Underside reflections of teleseismic shear waves at the two upper mantle seismic discontinuities, phases that appear on seismograms as precursors to the surface-reflected SS-wave (Fig. 2), are commonly used in mapping globally the topography of the two discontinuities [16,17]. High seismicity around the Pacific makes the south-central Pacific one of the regions most densely sampled by SS precursors. We used seismograms from earthquakes between 1990 and 1999 recorded by the Global Seismic Network of the Incorporated Research Institutions for Seismology (IRIS) and several regional seismic networks. Regional networks included the broadband seismic network for Fundamental Research on Earthquakes and Earth's Interior Anomaly (FREESIA) in Japan, the Broadband Andean Joint (BANJO) Experiment, and the Brazilian Lithospheric Seismic Project (BLSP94). The FREESIA network has been operated by the National Research Institute for Earth Science and Disaster Prevention, Japan, since 1994. BANJO was a portable broadband

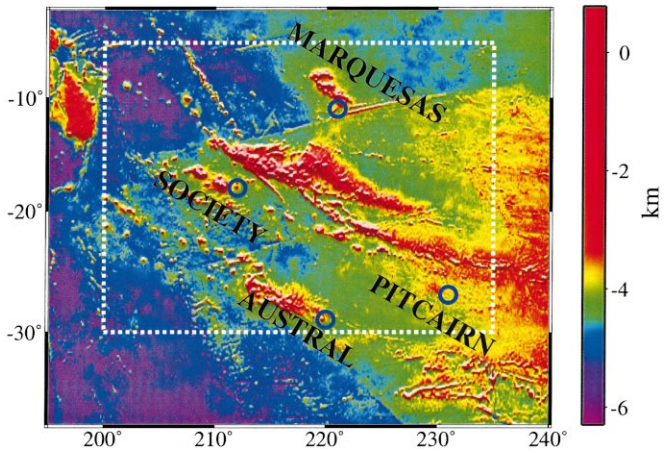

Fig. 1. Bathymetric map of the south-central Pacific [45] in the vicinity of the Pacific Superswell [1], approximately delineated by the dashed box. The positions of the Marquesas, Pitcairn, Society, and Macdonald hotspots [46] are indicated by blue circles.

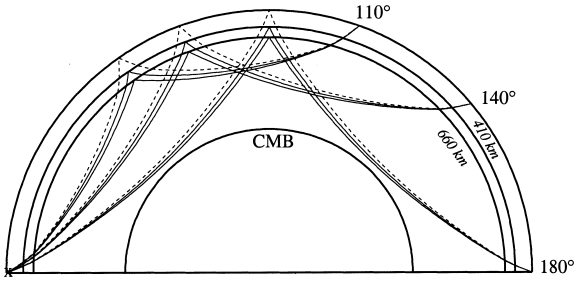

Fig. 2. Illustrative wave paths of the surface-reflected SS-phase, as well as precursors $S_{410}S$ and $S_{660}S$, at epicentral distances of 110, 140 and 180°. The travel time differences between SS and its precursors constrain the depths of the mantle discontinuities at the reflection points.

network operated by the Carnegie Institution of Washington and the University of Arizona in Chile, Peru, and Bolivia during 1994 and 1995. BLSP94 was another portable broadband network operated in Brazil by the Carnegie Institution of Washington and the Universidade de São Paulo from 1992 to 1995. We checked more than 10 000 transverse-component seismograms, and we selected a total of 2124 high-quality SS-waveforms with reflection points in the Superswell and surrounding regions, in the epicentral distance range 110–180°.

To each of the selected seismograms we first applied a 25–100-s bandpass filter, and we then deconvolved from each trace the waveform of the SS phase. To image lateral variations in the depths of the two seismic discontinuities, we binned the reflection points geographically. Instead of fixing the size of the binning areas [16,17], we varied the radius of the cap-shaped binning area and the number N of reflection points within the cap to improve the horizontal resolution in densely sampled regions. The value for N, 50–100 depending on the signal-to-noise ratio of seismograms for a given binning area, was chosen so that reflections from the two discontinuities were clearly visible. The radii of the binning caps lie mainly between 3° and 8° and average 5.5°.

For a reflection depth d, we calculated the arrival time of the underside reflection from that depth (S_dS) relative to SS for all N seismograms within a cap according to a standard global Earth model [18]. We then summed the N seismograms within a 1-s window centered on the arrival time of S_dS using an n^{th}-root stacking method [19]. We chose $n=4$ to reduce the uncorrelated noise relative to the usual linear stack ($n=1$). We varied d from 300 to 1000 km in increments of 1 km. The depth of a given discontinuity (d_{ij}) was first estimated using a bootstrap method [20] and caps of variable radius R_{ij} centered at the nodes of a large-meshed grid of size $L\times L°$. These depth values were further interpolated ($\tilde{d}_{kl}$) onto a $1\times1°$ grid by applying a weighted average among d_{ij}:

$$\tilde{d}_{kl}=\sum_{ij}w_{ijkl}d_{ij}/\sum_{ij}w_{ijkl}$$

where

$$w_{ijkl}=\begin{cases}1-r_{ijkl}/R_{ij}, \text{ if } r_{ijkl}\le R_{ij};\\ 0, \text{ if } r_{ijkl}>R_{ij}\end{cases}$$

and r_{ijkl} is the distance between two points on the $1\times1°$ and $L\times L°$ grids. We used $L=2$, 4, and 5. The smoothed images, however, are very similar over this range of large-grid spacing.

3. Results

The average thickness of the transition zone beneath the South Pacific Superswell and its surroundings (Fig. 3A) is 237 ± 5 km. This value is in approximate agreement with the average for the entire Pacific Ocean region derived by a similar method [16]. There is no difference in transition-zone thickness between the South Pacific Superswell (237 ± 5 km; dashed box in Fig. 3A) and the surrounding portion of our study area (237 ± 4 km).

The most prominent anomaly in transition-zone thickness beneath the South Pacific Superswell region lies near the Society hotspot. There the transition zone is only 213 ± 5 km thick over an area approximately 500×500 km (blue box in Fig. 3A) that is centered about 200 km to the southeast of the surface expression of the hotspot. The lateral scale of the anomalous region could be smaller

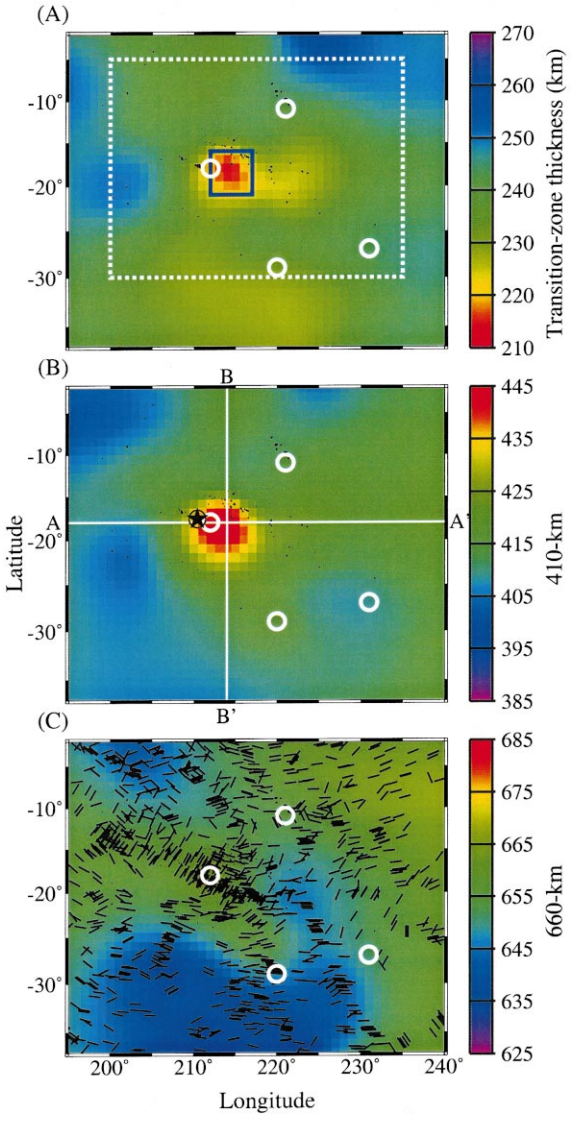

Fig. 3. Map view of (A) mantle transition-zone thickness, (B) the depth to the 410-km discontinuity, and (C) the depth to the 660-km discontinuity. The depths shown in (B) and (C) include corrections for the effects of departures in upper mantle velocity and crustal thickness from the standard Earth. The map outlines coincide with those of Fig. 1, as do the locations of surface hotspots (circles) and the approximate location of the South Pacific Superswell (dashed box). The region outlined in blue in (A) indicates an area of anomalously thin transition zone. The lines A–A′ and B–B′ in (B) denote the locations of the two profiles shown in Fig. 4A. The star in (B) indicates the location of Geoscope seismic station PPT, in Tahiti, and the black circle (1° radius) shows the approximate P-to-S conversion points of the teleseismic P410s phase at that station. The short line segments on (C) indicate azimuths of the S_{660}S-wave paths at the underside reflection points.
←

than that shown in Fig. 3, since the Fresnel zone for long-period SS precursors can be 1000 km or more [21], which serves to smooth the resolved topographic relief on the two discontinuities. A more spatially confined anomaly in transition-zone thickness would be greater in magnitude than that shown in Fig. 3 to produce the same observations.

We also show in Fig. 3 the inferred depths to the 410- and 660-km discontinuities beneath the South Pacific Superswell region. To derive these depths from the differential travel times between SS and S_dS, we must correct the SS travel times predicted by the standard model [18] for the upper mantle shear-wave velocity structure [22] and crustal thickness [23] across the region. The region has a thinner crust and a smaller upper mantle shear-wave velocity than the average Earth, but because these two contributions have opposite effects on the SS travel time, the corrections for mantle discontinuity depths are ≤ 10 km. Average values for the depths of the 410- and 660-km discontinuities in our study region are 413 ± 3 and 650 ± 3 km, respectively. The area of thinner transition zone near the Society hotspot corresponds to a depressed 410-km discontinuity (448 ± 4; Fig. 3B) and an almost flat 660-km discontinuity (661 ± 4 km; Fig. 3C). The depression of the 410-km discontinuity is associated with a weaker $S_{410}S$ phase than for reflection points far from the anomalous zone (Fig. 4A, boxed regions). The generally small amplitude of the $S_{410}S$ phases reflected near the Society hotspot could be the result of defocusing by a downward deflection of the discontinuity (Fig. 4B).

The depths to the 410- and 660-km discontinuities shown in Fig. 3 are likely to be biased by unmodeled aspects of the velocity structure of the upper mantle beneath the region. Because $S_{660}S$–$S_{410}S$ differential times are not sensitive to heterogeneities shallower than the 410-km discontinuity, the estimated transition-zone thickness is expected to be more accurate than the depths to

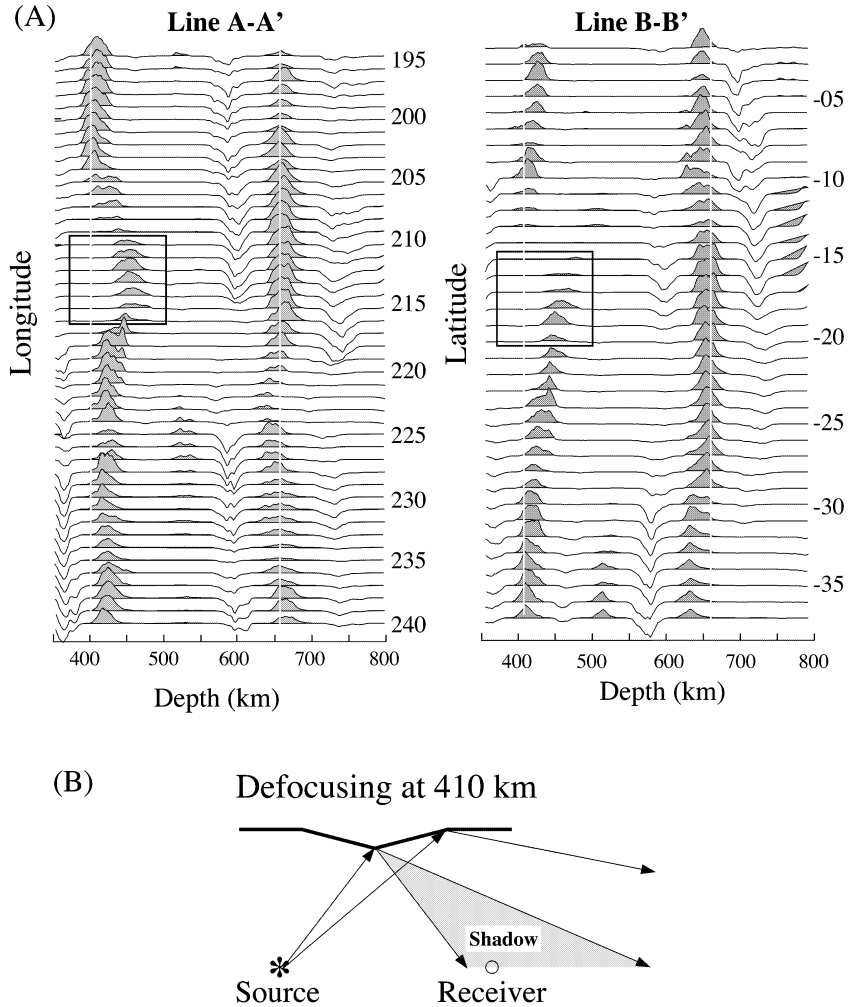

Fig. 4. (A) Two profiles of stacked traces along the lines A–A′ and B–B′ from Fig. 3B. Stacked waveforms are shown as a function of the reflection depth of the SS precursor. Vertical lines indicate reflections at depths of 410 and 660 km. Negative-polarity arrivals appearing at approximately 360, 590, and 730 km depth are side lobes of the 410- and 660-km reflections; some traces show evidence for a reflection at about 520 km depth. Boxes denote waveforms indicative of a depressed 410-km discontinuity; the reflection points of these waveforms lie within the blue box in Fig. 3A. Most of these $S_{410}S$-waveforms have lower amplitudes than those with reflection points outside of the anomalous area. (B) Schematic illustration of reflection at a downward-deflected 410-km discontinuity. A shadow zone of low reflected-wave amplitudes is predicted by ray theory.

the individual discontinuities. Our discussion below is therefore based primarily on the observed variations in mantle transition-zone thickness.

4. Discussion

The transition-zone thickness of the anomalous region near the Society hotspot is 24 ± 7 km less than that of the surrounding region and 29 ± 5 km less than that for the average Earth [16]. Such a large variation in transition-zone thickness has not previously been reported for the south-central Pacific. Instead, only small variations in the depths of the two discontinuities and about a 10-km thinner transition zone overall were obtained for this region in the most comparable global study of SS precursors [16]. Our different

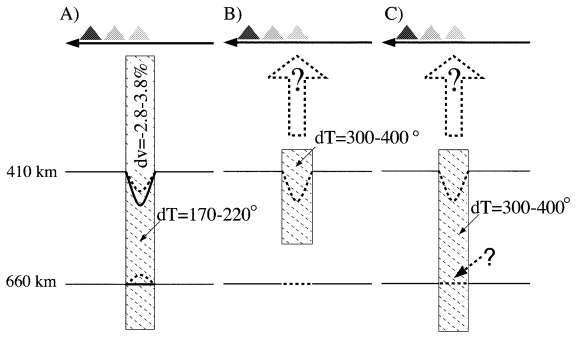

Fig. 5. Schematic illustration of three possible interpretations of our observations. The shaded regions represent hot material associated with a mantle plume beneath the Society hotspot. Solid and dashed lines indicate, respectively, the estimated and actual depths of the 410- and 660-km discontinuities. Vertical exaggeration is approximately 8:1. (A) The actual depths of the two discontinuities are about 10–15 km shallower than our estimates because of an unmodeled low-velocity anomaly that is confined to a narrow vertical conduit not resolvable by global tomographic imaging. Hot material rises from the lower mantle and continues to a region of decompression melting in the shallow upper mantle. (B) Our depth estimates reflect the actual depths of the two discontinuities, and hot mantle material is present only in the vicinity of the 410-km discontinuity. If this thermal anomaly is associated with the Society hotspot, any plume is likely a variable or transient feature rather than a continuous uniform conduit. (C) Our depth estimates reflect the actual depths of the two discontinuities, and the plume originates in the lower mantle. The lack of a deflection of the 660-km discontinuity despite the excess temperature could be due to a change in the nature of the phase boundary at high temperatures, an effect seen to date only in pure Mg_2SiO_4 [37,38].

result is likely due to a larger volume of data and a smaller cap size used for binning and stacking. Because the anomalous region is well sampled by our data set, the radii of binning caps we used for this feature were about 2.5°, while in the global study [16] a cap of 10° radius was used. When the dimension of the cap exceeds the lateral scale of an anomaly, stacking smooths the topographic relief at the discontinuity depth and yields an underestimate of the magnitude of lateral variations in transition-zone thickness. If we apply a uniform cap radius of 10° to our data, for instance, the thickness of the transition zone obtained for the anomalous region is 231 ± 5 km, nearly the same as the rest of the study area.

In principle, the area of anomalously thin transition zone could also be detected by the differential travel times between teleseismic P-waves and P-to-S conversions at the discontinuity [12,13]. Detection of such converted phases may require seafloor observations, however. The center of the observed anomaly lies about 300 km from the nearest permanent seismometer, Geoscope station PPT [24] (Fig. 3B), whereas the points of conversion of P-to-S at 410 km depth (P410s) are generally less than 100 km from the station (black circle in Fig. 3B).

The anomalously thin transition zone beneath the Society hotspot may be converted to an excess temperature if we assume that the perturbations to discontinuity depths are thermal in origin and that temperature anomalies within the transition zone are vertically coherent. The conversion depends on the values of the Clapeyron slopes for the two phase boundaries. Reported estimates of the Clapeyron slopes from both experimental and theoretical studies, however, show a wide range of values: approximately 1.5–2.9 [14,25,26] and −4.0 to −2.0 [15,27,28] MPa/°C for the 410- and 660-km phase transitions, respectively. With more recent thermodynamic data and equations of state, Bina and Helffrich [29] re-evaluated earlier experimental data and found that the implied values of Clapeyron slopes are more nearly consistent. On the basis of their discussion, we adopt 2.5–2.9 and −3.0 to −2.0 MPa/°C as values that likely bracket the Clapeyron slopes for the phase transitions at 410 and 660 km depth, respectively.

The excess temperature implied by these values for Clapeyron slopes is 170–220°C. For such an excess temperature, the 410- and 660-km discontinuities should be at 433–438 km and 645–650 km depth, respectively, each about 10–15 km shallower than our estimates. This discrepancy may be a consequence of an undercorrection for the velocity heterogeneity in the upper mantle in the vicinity of the anomaly (Fig. 5A). In the three-dimensional model used to correct the upper mantle contribution to the SS travel time [22], the upper mantle overlying the anomalous transition zone and that in the surrounding region are respectively 0.8 and 1.2% slower on average than normal mantle. For comparison, the S-wave velocity is about 3% lower than surrounding values

within the mantle plume imaged beneath the Iceland hotspot [11]. Reducing the upper mantle shear velocity by 2% results in a shoaling by about 10 km in the depths of the two mantle discontinuities. The depths of the 410- and 660-km discontinuities beneath the Society hotspot can be made consistent with a thermal origin for the transition-zone thickness anomaly if the average shear velocity of the upper mantle in the vicinity of the hotspot is about 1.6–2.6% less than for surrounding regions (i.e. 2.8–3.8% less than the average Earth). Such an upper mantle velocity anomaly is consistent with the observation that seismic stations in Tahiti have a large teleseismic P-wave travel time delay ($\sim$1.3 s) compared with nearby stations ($\sim$0.8 s) [30]. A narrow plume of low seismic velocities in the upper mantle cannot be resolved, however, in existing mantle tomographic images for the region, but additional stations planned for this region [31,32] may yield upper mantle velocity images of sufficient resolution to confirm such a structure.

If the correction for upper mantle velocity has been made correctly, in contrast, and our estimates for the depths of the two seismic discontinuities are close to the actual depths, then alternative interpretations are possible. The temperature anomaly may be restricted to a depth interval that contains the 410-km discontinuity but not the 660-km discontinuity (Fig. 5B), or the horizontal extent of any temperature anomaly at 660 km depth may be too small to resolve. Such a pattern might be the result of episodic variations in the width of a plume conduit [33] or one or more transient plumes, similar to those seen in high-Rayleigh-number convection in laboratory fluids [34,35]. The heads of transient plumes observed in laboratory experiments have lateral extents up to four to five times those of the tails [35], and episodic variations in the radius of a plume conduit can span a comparable factor [33]. The source of such a transient or episodic plume could be at any depth greater than 410 km, including either the base of the transition zone or the core–mantle boundary.

There are several difficulties with this interpretation, however. If the transition-zone thickness anomaly is explained entirely by a deflection in the 410-km discontinuity, then a rather large excess temperature of 300–400°C at that depth (Fig. 5B) is implied [29]. Such a temperature anomaly could not extend at the same lateral dimension to 660 km (because, by assumption, that discontinuity is not visibly perturbed) or to depths much shallower than 410 km (because the correction for upper mantle velocity would then need to be raised, which would raise the depths of the discontinuities). If the lateral extent of the temperature anomaly is $\sim$500 km, then the ratio of its vertical to its horizontal dimensions is substantially less than unity, contrary to the form of episodic variations in plume conduit width seen in the laboratory [33] and the more equant dimensions of plume heads in high-Rayleigh-number experiments [34,35]. Interaction of a rising plume with the lithosphere would tend to broaden the thermal anomaly, but this effect would be more than offset by a low-viscosity asthenosphere, which would act to narrow the width of upwelling flow. The lateral extent of the transition-zone anomaly, as noted above, may be less than 500 km, but a lesser horizontal dimension would increase the magnitude of the topographic relief on the 410-km discontinuity, raising the implied temperature further.

A large downward deflection of the 410-km discontinuity and a 'normal' 660-km discontinuity could have another explanation. If the normal temperature at the base of the upper mantle is about 1600°C [36], and if the 300–400°C excess temperature at 410 km depth is extended downward along an adiabat, then the temperature at the 660-km discontinuity could be as great as 1900–2000°C. Limited data for pure Mg_2SiO_4 indicate that at these conditions there is a direct phase change from β-Mg_2SiO_4 to perovskite plus magnesiowüstite [37]. The transition is thought to be characterized by a positive Clapeyron slope, and the triple point lies near 23 GPa, 1850°C [37]. The 660-km discontinuity might therefore appear to be at or near a 'normal' depth despite a high excess temperature (Fig. 5C). Such an explanation, however, requires either a large Clapeyron slope or a reduction by several hundred degrees in the temperature at the triple point, either of which is unlikely, given the existing min-

eralogical data. Phase relations in multi-component pyrolite, however, display a more complex temperature dependence [38]; the quantitative viability of this explanation thus remains to be demonstrated experimentally. A corollary to this explanation is that the 300–400°C excess temperature cannot continue to shallow depths in the upper mantle, lest the correction to SS travel times for upper mantle velocity raise the discontinuity depths to shallower levels, as with the case in Fig. 5A. Any plume beneath the Society hotspot is therefore discontinuous, as with the case in Fig. 5B, but the vertical extent of the hot material straddling the transition zone would be greater than that case and could extend into the lower mantle.

Of the interpretations depicted in Fig. 5, the first (A) is the most straightforward and the most consistent with observations of mantle seismic structure at other major hotspots [10–12]. The second (B) interpretation calls for a pronounced thermal anomaly having a pancake shape not easily reconciled with expectations from fluid dynamical experiments. Both the second and third (C) interpretations invoke deep-seated thermal anomalies not clearly linked to the upper mantle melt generation responsible for the island and seamount chain.

Of the four hotspots within the region of the South Pacific Superswell, our observations are consistent with a classical mantle plume [6] only for the Society hotspot (Figs. 3A and 5A). Our data set has poor resolution in the immediate vicinity of the Pitcairn hotspot, but the transition zone is well sampled beneath the Macdonald and Marquesas hotspots (Fig. 3C). It is not immediately evident why the mantle structure beneath the Society, Macdonald, and Marquesas hotspots should differ so substantially. Under the assumption that all three hotspots are underlain by plumes, estimates of the plume buoyancy flux derived from residual bathymetry and geoid anomalies [39,40] do not differ by more than a factor of 3, although the Society track has produced islands with the largest total area among the four hotspots. Measured $^{3}He/^{4}He$ ratios in basalts from the Society and Austral (as well as Pitcairn) hotspot tracks are not markedly different from one another [41]. If each of the hotspots is underlain by an episodic or a transient plume (Fig. 5B,C), or by several transient plumes following a common upward trajectory, then it is possible that there is presently a plume head or a wide plume conduit near the depth of the mantle transition zone beneath the Society hotspot but not beneath the other two.

On the other hand, there are differences among these three hotspots that may pertain to differences in deep structure. The Society hotspot displays a reasonably well-defined age progression as well as active volcanism at its southeastern terminus [42]. Shear-wave splitting observations [43] indicate that the upper mantle beneath Tahiti, at the edge of the Society hotspot (Fig. 3A), distinguishes itself from the mantle beneath other islands in the region by a lack of azimuthal anisotropy, as would be expected for primarily vertical flow. In contrast, the Marquesas chain is comparatively short, ages depart from a simple linear progression, and there is no known site of active volcanism [3]. The wide range of ages and lack of a clear age progression along the Austral–Cook chain, thought to be linked to the Macdonald hotspot, led McNutt et al. [2] to favor lithospheric stress and shallow melt generation rather than a mantle plume as the explanation for most volcanism along this archipelago. These differences may be signatures of different mantle upwelling patterns beneath the three hotspots.

The fact that we observe a normal transition-zone thickness beneath the South Pacific Superswell as a whole suggests that the long-wavelength seismic anomaly in the underlying lower mantle – the so-called Pacific Superplume [8] – does not involve transport of heat into the upper mantle at comparable horizontal scales. The South Pacific Superswell may nonetheless derive some dynamic support for its generally shallow seafloor from a broad pattern of lower mantle upwelling, in the manner proposed for the elevated terrain of southern Africa [10,44]. With or without such lower mantle support of topography, the pervasive volcanism across the South Pacific Superswell must be primarily an upper mantle phenomenon, a consequence of a broad area of somewhat higher temperatures and melt generation rates than

normal [1,2], except for the presence of at least one narrow plume likely originating from the lower mantle.

Acknowledgements

We are grateful for helpful discussions with Yingwei Fei, Erik Hauri, Masayuki Obayashi, Mark Richards, Selwyn Sacks, and Lianxing Wen, and we thank IRIS and FREESIA for providing seismic waveform data. Emile Okal, Justin Revenaugh, and an anonymous reviewer provided constructive reviews that improved the manuscript significantly. *[RV]*

References

[1] M.K. McNutt, K.M. Fischer, The South Pacific superswell, in: B.H. Keating, P. Fryer, R. Batiza, G.W. Boehlert (Eds.), Seamounts, Islands, and Atolls, Geophysical Monograph Series, Vol. 43, American Geophysical Union, Washington, DC, 1987, pp. 25–43.

[2] M.K. McNutt, D.W. Caress, J. Reynolds, K.A. Jordahl, R.A. Duncan, Failure of plume theory to explain midplate volcanism in the southern Austral islands, Nature 389 (1997) 479–482.

[3] A.E. Gripp, R.G. Gordon, Young tracks of hotspots and current plate velocities relative to the hotspots, Geophys. J. Int. (2002) in press.

[4] E.A. Okal, R. Batiza, Hotspots: the first 25 years, in: B.H. Keating, P. Fryer, R. Batiza, G.W. Boehlert (Eds.), Seamounts, Islands, and Atolls, Geophysical Monograph Series, Vol. 43, American Geophysical Union, Washington, DC, 1987, pp. 1–11.

[5] V. Clouard, A. Bonneville, How many Pacific hotspots are fed by deep-mantle plumes?, Geology 29 (2001) 695–698.

[6] W.J. Morgan, Convection plumes in the lower mantle, Nature 230 (1971) 42–43.

[7] W.J. Su, R.L. Woodward, A.M. Dziewonski, Degree 12 model of shear velocity heterogeneity in the mantle, J. Geophys. Res. 99 (1994) 6945–6980.

[8] Y. Fukao, Seismic tomogram of the Earth's mantle: geodynamic implications, Science 258 (1992) 625–630.

[9] A. Cazenave, C. Thoraval, Mantle dynamics constrained by degree 6 surface topography, seismic tomography and geoid: inference on the origin of the South Pacific Superswell, Earth Planet. Sci. Lett. 122 (1994) 207–219.

[10] C. Lithgow-Bertelloni, P.G. Silver, Dynamic topography, plate driving forces and the African superswell, Nature 395 (1998) 269–272.

[11] C.J. Wolfe, I.T. Bjarnason, J.C. Van Decar, S.C. Solomon, Seismic structure of the Iceland mantle plume, Nature 385 (1997) 245–247.

[12] Y. Shen, S.C. Solomon, I.Th. Bjarnason, C.J. Wolfe, Seismic evidence for a lower-mantle origin of the Iceland plume, Nature 395 (1998) 62–65.

[13] X. Li, R. Kind, K. Priestley, S.V. Sobolev, F. Tilmann, X. Yuan, M. Weber, Mapping the Hawaiian plume conduit with converted seismic waves, Nature 405 (2000) 938–941.

[14] T. Katsura, E. Ito, The system Mg_2SiO_4-Fe_2SiO_4 at high pressures and temperatures: precise determination of stabilities of olivine, modified spinel, and spinel, J. Geophys. Res. 94 (1989) 15663–15670.

[15] E. Ito, E. Takahashi, Postspinel transformations in the system Mg_2SiO_4–Fe_2SiO_4 and some geophysical implications, J. Geophys. Res. 94 (1989) 10637–10646.

[16] M.P. Flanagan, P.M. Shearer, Global mapping of the topography on the transition zone velocity discontinuities by stacking SS precursors, J. Geophys. Res. 103 (1998) 2673–2692.

[17] Y. Gu, A.M. Dziewonski, C.B. Agee, Global de-correlation of the topography of transition zone discontinuities, Earth Planet. Sci. Lett. 157 (1998) 57–67.

[18] B.L.N. Kennett, E.R. Engdahl, Travel times for global earthquake location and phase identification, Geophys. J. Int. 105 (1991) 429–465.

[19] E.R. Kanasewich, Time Sequence Analysis in Geophysics, University of Alberta Press, Edmonton, AB, 1973, 364 pp.

[20] B. Efron, R. Tibshirani, Bootstrap methods for standard errors, confidence intervals, and other measures of statistical accuracy, Stat. Sci. 1 (1986) 54–75.

[21] F. Neele, H. de Regt, J.C. Van Decar, Gross errors in upper-mantle discontinuity topography from underside reflection data, Geophys. J. Int. 129 (1997) 194–204.

[22] X.-F. Liu, A.M. Dziewonski, Global analysis of shear wave velocity anomalies in the lowermost mantle, in: M. Gurnis, M.E. Wysession, E. Knittle, B.A. Buffett (Eds.), The Core-Mantle Boundary Region, Geodynamics Series, Vol. 28, American Geophysical Union, Washington, DC, 1998, pp. 21–36.

[23] W.D. Mooney, G. Laske, G. Masters, Crust 5.1: A global crustal model at 5×5 degrees, J. Geophys. Res. 103 (1998) 727–747.

[24] L. Vinnik, S. Chevrot, J.-P. Montagner, Evidence for a stagnant plume in the transition zone?, Geophys. Res. Lett. 24 (1997) 1007–1010.

[25] M. Akaogi, E. Ito, A. Navrotsky, Olivine-modified spinel–spinel transitions in the system Mg_2SiO_4–Fe_2SiO_4: calorimetric measurements, thermochemical calculation, and geophysical application, J. Geophys. Res. 94 (1989) 15671–15685.

[26] A. Chopelas, Thermal properties of β-Mg_2SiO_4 at mantle pressures derived from vibrational spectroscopy: implications for the mantle at 400 km depth, J. Geophys. Res. 96 (1991) 11817–11829.

[27] E. Ito, M. Akaogi, L. Topor, A. Navrotsky, Negative

pressure-temperature slopes for reactions forming $MgSiO_3$ perovskite from calorimetry, Science 249 (1990) 1275–1278.
[28] M. Akaogi, E. Ito, Refinement of enthalpy measurement of $MgSiO_3$ perovskite and negative pressure-temperature slopes for perovskite-forming reactions, Geophys. Res. Lett. 20 (1993) 1839–1842.
[29] C.R. Bina, G. Helffrich, Phase transition Clapeyron slopes and transition zone seismic discontinuity topography, J. Geophys. Res. 99 (1994) 15853–15860.
[30] A.M. Dziewonski, D.L. Anderson, Travel times and station corrections for P waves at teleseismic distances, J. Geophys. Res. 88 (1983) 3295–3314.
[31] M. Ishida, S. Maruyama, D. Suetsugu, S. Matsuzaka, T. Eguchi, Superplume Project: towards a new view of whole Earth dynamics, Earth Planets Space 51 (1999) i–v.
[32] G. Barruol, A. Tommasi, D. Bosch, V. Clouard, E. Debayle, M.-P. Doin, M. Godard and C. Thoraval, POLYNESIA 2001: structure and dynamics of the upper mantle beneath French Polynesia, in: The 7th Workshop on 'Numerical Modeling of Mantle Convection and Lithospheric dynamics', 2001, p. 52.
[33] P. Olson, U. Christensen, Solitary wave propagation in a fluid conduit within a viscous matrix, J. Geophys. Res. 91 (1986) 6367–6374.
[34] M. Manga, D. Weeraratne, Experimental study of non-Boussinesq Rayleigh-Benard convection at high Rayleigh and Prandtl numbers, Phys. Fluids 11 (1999) 2969–2976.
[35] C. Lithgow-Bertelloni, M.A. Richards, C.P. Conrad, R.W. Griffiths, Plume generation in natural thermal convection at high Rayleigh and Prandtl numbers, J. Fluid Mech. 434 (2001) 1–21.
[36] E. Ito, T. Katsura, A temperature profile of the mantle transition zone, Geophys. Res. Lett. 16 (1989) 425–428.
[37] Y. Fei, C.M. Bertka, Phase transitions in the Earth's mantle and mantle mineralogy, in: Y. Fei, C.M. Bertka, B.O. Mysen (Eds.), Mantle Petrology: Field Observations and High Pressure Experimentation: A Tribute to Francis R. (Joe) Boyd, Geochemical Society, Houston, TX, 1999, pp. 189–207.
[38] K. Hirose, Phase transitions in pyrolitic mantle around 670-km depth: Implications for upwelling of plumes from the lower mantle, J. Geophys. Res. (2002) in press.
[39] G.F. Davies, Ocean bathymetry and mantle convection, 1, large-scale flow and hotspots, J. Geophys. Res. 93 (1988) 10467–10480.
[40] N.H. Sleep, Hotspots and mantle plumes: Some phenomenology, J. Geophys. Res. 95 (1990) 6715–6736.
[41] P.E. van Keken, E.H. Hauri, C.J. Ballentine, Mantle mixing: the generation, preservation and destruction of chemical heterogeneity, Annu. Rev. Earth Planet. Sci. (2002) in press.
[42] J. Talandier, G.T. Kuster, Seismicity and submarine volcanic activity in French Polynesia, J. Geophys. Res. 81 (1976) 936–948.
[43] R.M. Russo, E.A. Okal, Shear wave splitting and upper mantle deformation in French Polynesia: evidence for small-scale heterogeneity related to the Society hotspot, J. Geophys. Res 103 (1998) 15089–15107.
[44] S.S. Gao, P.G. Silver, K.H. Liu, the Kaapvaal Seismic Group, Mantle discontinuities beneath southern Africa, Geophys. Res. Lett. (2002) in press.
[45] W.H.F. Smith, D.T. Sandwell, Global sea floor topography from satellite altimetry and ship depth soundings, Science 277 (1997) 1957–1962.
[46] M.A. Richards, B.H. Hager, N.H. Sleep, Dynamically supported geoid highs over hotspots: observation and theory, J. Geophys. Res. 93 (1988) 7690–7708.